

The RAVEN - Design and Validation of a Telesurgery System

Mitchell J.H. Lum*, Diana C.W. Friedman*, Jacob Rosen*, Ganesh Sankaranarayanan*,
Hawkeye King*, Kenneth Fodero II*, Rainer Leuschke*, Mika N. Sinanan[†], and Blake
Hannaford*

*Department of Electrical Engineering, BioRobotics Lab

[†]Department of Surgery, Center for Video Endoscopic Surgery

University of Washington, Seattle, WA 98195

Email: <mitchlum, dwarden, rosen, ganeshs, hawkeye1, kfodero, rainer, mssurg,
blake>@u.washington.edu

Abstract

The collaborative effort between fundamental science, engineering and medicine provides physicians with improved tools and techniques for delivering effective health care. Minimally invasive surgery (MIS) techniques have revolutionized the way a number of surgical procedures are performed. Recent advances in surgical robotics are once again revolutionizing MIS interventions and open surgery. In an earlier research endeavor, thirty surgeons performed seven different MIS tasks using the Blue Dragon system to collect measurements of position, force, and torque on a porcine model. This data served as the foundation for a kinematic optimization of a spherical surgical robotic manipulator. Following the optimization, a 7-DOF cable-actuated surgical manipulator was designed and integrated, providing all degrees of freedom present in manual MIS as well as wrist joints located at the surgical end-effector. The RAVEN surgical robot system has the ability to teleoperate utilizing a single bi-directional UDP socket via a remote master device. Preliminary telesurgery experiments were conducted using the RAVEN. The experiments illustrated the system's ability to operate in extreme conditions using a variety of network settings.

1. INTRODUCTION

Innovation in surgery allows surgeons to provide better health care to their patients. In particular, minimally invasive surgery (MIS) reduces postoperative hospital stays to just over a day compared to more

1 than a week when the procedure is performed ‘open’ [Robinson and Stiegmann, 2004]. More precise, less
2 invasive and inherently safer techniques and equipment are a natural part of the evolution of healthcare.
3 In April 1985, Kwoh and colleagues used a Unimation Puma 200 robot to orient a biopsy needle for
4 neurosurgery, marking the first use of robotics in surgery [Kwoh et al., 1988]. The latter half of the 1980s
5 also saw the development of the system that would later become ROBODOC, which was used for precision
6 bone machining for orthopedic surgeries such as cement-less total hip replacements first in canines and
7 then in humans [Taylor et al., 1994], [Taylor et al., 1989], as well as the use of a robot to perform a
8 transurethral resection of the prostate, first with a Unimate Puma 560 and later with the specially designed
9 Probot [Davies, 2000], [Davies et al., 1989], [Harris et al., 1997]. The use of robotics in surgery increased
10 in popularity in the 1990s, with devices such as the SRI telepresence system [Hill et al., 1994], the IBM
11 Research Center/Johns Hopkins University surgical robot [Taylor et al., 1995], the system designed at the
12 Politecnico di Milano in Italy [Rovetta et al., 1996], and the Black Falcon from Massachusetts Institute
13 of Technology [Madhani et al., 1998].

14 The Automated Endoscopic System for Optimal Positioning (AESOP) was the first robot approved for
15 use in surgery by the US Food and Drug Administration (FDA). After its approval in 1994, the system
16 assisted surgeons by supporting an endoscope and repositioning according to the surgeons’ instructions
17 [Jacobs, 1997], [Sackier et al., 1997]. Licensed by Computer Motion, Inc. (Goleta, CA), the AESOP was
18 later incorporated into the Zeus robotic surgery system [Ghodoussi et al., 2002], which received FDA
19 approval in September 2002. The Zeus was used in the first transatlantic telesurgery, performed between
20 Manhattan, New York, USA and Strasbourg, France [Ghodoussi et al., 2002], [Marescaux et al., 2001].
21 The Zeus’s major competitor was the da Vinci surgical robot, produced by Intuitive Surgical, Inc. (Moun-
22 tain View, CA) and FDA approved in July 2000 [Guthart and Salisbury, 2000]. In June 2003, the com-
23 panies merged under the name Intuitive Surgical, Inc. and production of the Zeus and AESOP sys-
24 tems ceased [Sim et al., 2006]. Other commercially available systems include the NeuroMate (which,
25 along with ROBODOC, was produced by Integrated Surgical Systems, Inc. in Davis, CA, until 2005)
26 [Cleary and Nguyen, 2001], [Lavallée et al., 1992] and the Naviot laparoscope manipulator (Hitachi Co.,
27 Japan) [Kobayashi et al., 1999].

28 Several surgical robotic systems are currently in development around the world. The system designed
29 at the University of Tokyo [Mitsuishi et al., 2003] has performed telesurgical experiments throughout
30 Asia. The NeuRobot [Hongo et al., 2002] has been used in clinical applications. Other systems include

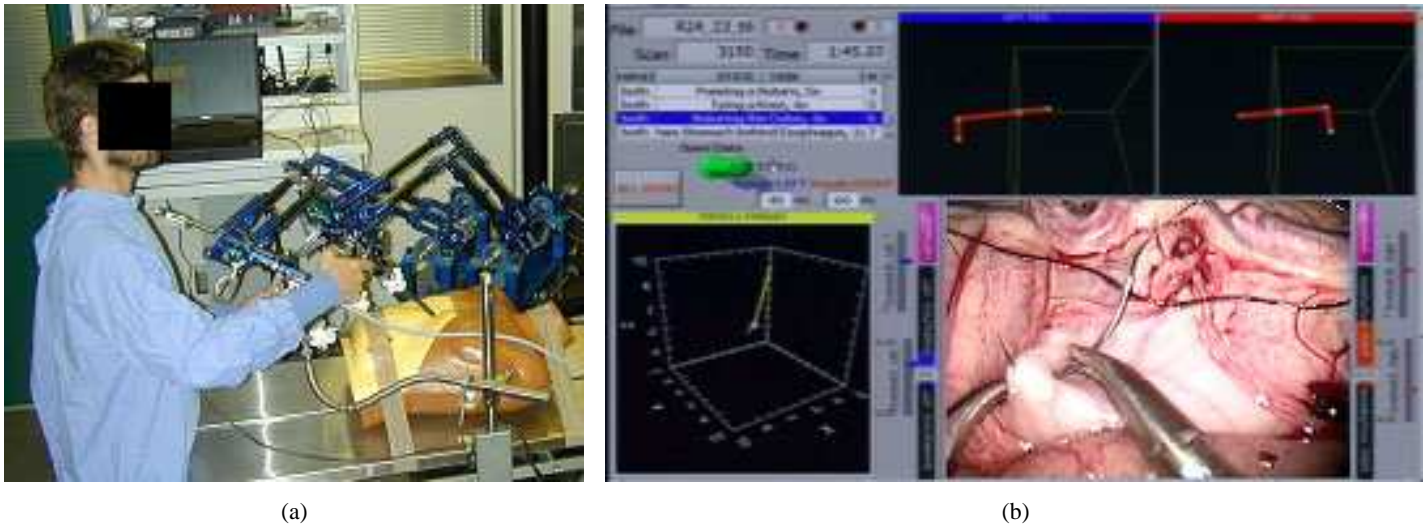


Fig. 1. The Blue Dragon system. (a) The system integrated into a minimally invasive surgery operating room. (b) Graphical user interface shows the position and orientation of each tool with respect to the port as well as an overlaid video feed from the endoscope.

1 the Berkeley/UCSF laparoscopic telesurgical workstation [Cavusoglu et al., 2003], the Light Endoscopic
 2 Robot [Berkelman et al., 2003], and the MC^2E [Zemiti et al., 2007].

3 The University of Washington's RAVEN differs from previous systems because the design originated
 4 from a long standing relationship with surgeons. The collaborative effort spawned an engineering approach,
 5 applied to surgery resulting in *in-vivo* measurements that quantified the tool-tissue interactions. The
 6 RAVEN manipulator is optimized based on this surgical data and validation studies using the Society of
 7 American Gastrointestinal Endoscopic Surgeons (SAGES) Fundamentals of Laparoscopic Surgery (FLS)
 8 skills tasks give results that are meaningful in the surgical context. This paper will discuss the design,
 9 development, and accomplishments of the RAVEN Surgical Robot.

10 2. CLINICAL REQUIREMENTS

11 For over a decade and a half, strong collaboration between engineers in the BioRobotics Lab and
 12 surgeons in the Center for Video Endoscopic Surgery has focused on answering clinically relevant
 13 problems. Surgical training followed the mentor/student model whereby the expert surgeon shows a
 14 novice how to perform a task and the novice then mimics the expert. The evaluation of surgical skill
 15 has historically been a subjective process.

16 In order to move toward more objective measures, extensive work has been performed in the area
 17 of surgical measurement and skill assessment [Rosen et al., 2006]. The Blue Dragon, a passive device
 18 instrumented with sensors, was developed for measuring surgical tool displacements, forces and torques
 19 during *in-vivo* animal surgeries (Figure 1). Using the Blue Dragon, an extensive database was created

1 of *in-vivo* tissue handling/examination, dissection and suturing tasks performed by 30 surgeons. Analysis
2 of this data indicated that 95% of the time the surgical tools were located within a conical range of
3 motion with a vertex angle 60° (termed the dexterous workspace, DWS). A measurement taken on a
4 human patient showed that in order to reach the full extent of the abdomen, the tool needed to move 90°
5 in the mediolateral (left to right) and 60° in the superior/inferior direction (head to foot). The extended
6 dexterous workspace (EDWS) was defined as a conical range of motion with a vertex angle of 90° and is
7 the workspace required to reach the full extent of the human abdomen without reorientation of the base of
8 the robot. These parameters, obtained through surgical measurement, served as a basis for the kinematic
9 optimization of the RAVEN spherical mechanism.

10 3. ROBOT DESIGN

11 The RAVEN Surgical Robot consists of three main pieces: the patient site, the surgeon site and a
12 network connecting the two. Using the typical teleoperator system nomenclature the surgeon site is the
13 ‘master’ and the patient site is the ‘slave’. The patient site consists of two surgical manipulators that are
14 positioned over the patient. The surgeon site consists of two control devices and a video feed from the
15 operative site. The communication layer can be any TCP/IP network including a local private network,
16 the Internet or even a wireless network.

17 3.1. The Patient Site

18 Much of the engineering effort was focused on developing the patient site. Starting with the range of
19 motion required for surgery, the spherical mechanism was analyzed and optimized for this application
20 [Lum et al., 2006]. The optimization determined the most compact mechanism with the best kinematic
21 performance in the workspace required for surgery. Once the optimal geometry of the mechanism was
22 determined, a detailed design of the arms and tool interface was performed to yeild a lightweight and
23 rigid pair of manipulators.

24 3.1.1. Design Approach: The pivot point constraint in MIS makes the spherical manipulator a natural
25 candidate for a surgical robot. The CMI Zeus system used a SCARA-like manipulator and required an
26 MIS port to constrain its motion. A spherical mechanism inherently allows rotation about a remote center
27 requiring neither a physical constraint nor a complex controller to prevent tangential motion or forces
28 about the incision. The spherical mechanism would allow the robot to be operated under both minimally
29 invasive and ‘open’ surgery configurations with no change to the system whatsoever.

1 An adjustable passive aluminum mock-up was fabricated to model the kinematics of the spherical
2 manipulator in parallel and serial configurations. The link angles of the spherical mechanism are the angles
3 between adjacent revolute joints. The base angle is the angle between the two most proximal revolute joints
4 of the parallel manipulator, which would be the two actuated joints for the robotic mechanism. The mock-
5 up was designed such that a standard MIS tool with 5mm shaft could pass through the distal joint. In a
6 dry-lab set-up, a number of kinematic configurations were compared on a training torso (Simulab, Seattle,
7 WA) to assess range of motion and collision problems. These dry-lab experiments showed that a parallel
8 configuration had a limited workspace with kinematic singularities contained in the workspace, self-
9 collision problems (where an arm collided with itself), robot-robot collisions (between two robots within
10 the surgical scene) and robot-patient collisions (Figure 2). Based on some of these practical constraints it
11 was determined that the best configuration was two serial manipulators.

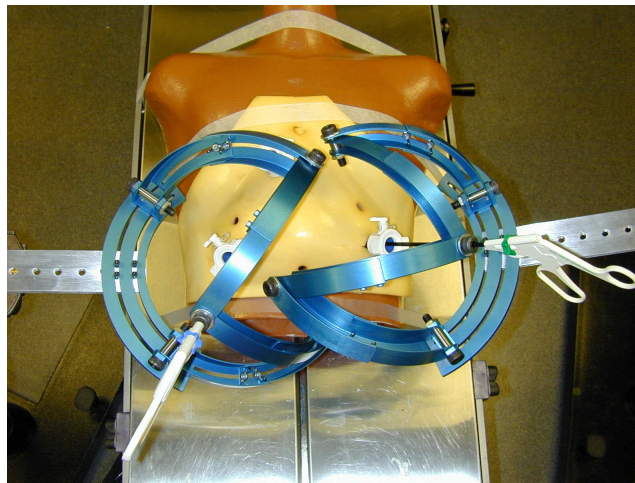


Fig. 2. Two parallel mechanism aluminum mock-ups. The parallel mechanism has four links and would have two actuated joints (the two base joints) if used for a surgical robot. It is clear from this picture that the parallel mechanism suffers from collision problems. The dry-lab experiments underscored the need for the most compact mechanism possible.

12 The wet-lab experiment applied results from the dry-lab experiment; two serial manipulators were
13 evaluated with surgeons performing suturing and tissue handling tasks *in-vivo* on a porcine model as
14 shown in Figure 3. For this evaluation the link angles were set to 75° and the surgeons were able to
15 perform all the required tasks without robot-robot or robot-patient collisions. The wet-lab experiment
16 validated that two serial spherical manipulators in the surgical scene would be feasible for a surgical
17 robotic system.

18 A detailed numerical analysis in [Lum, 2004] analyzed both the parallel and serial mechanism and
19 confirmed the results of the experimental evaluation. A kinematic optimization was performed to determine



Fig. 3. (a) Close-up photo of two serial mechanisms in the wet-lab set-up. (b) Surgeons manipulating conventional tools inserted through the last axis of the mock-ups using the serial configuration.

1 the optimal link angles based on the workspace required for surgery. One striking result is that for base
 2 angles greater than zero (both joint axes collinear), the parallel mechanism is plagued by an area of
 3 kinematic singularity within the center of its workspace (Figure 4).

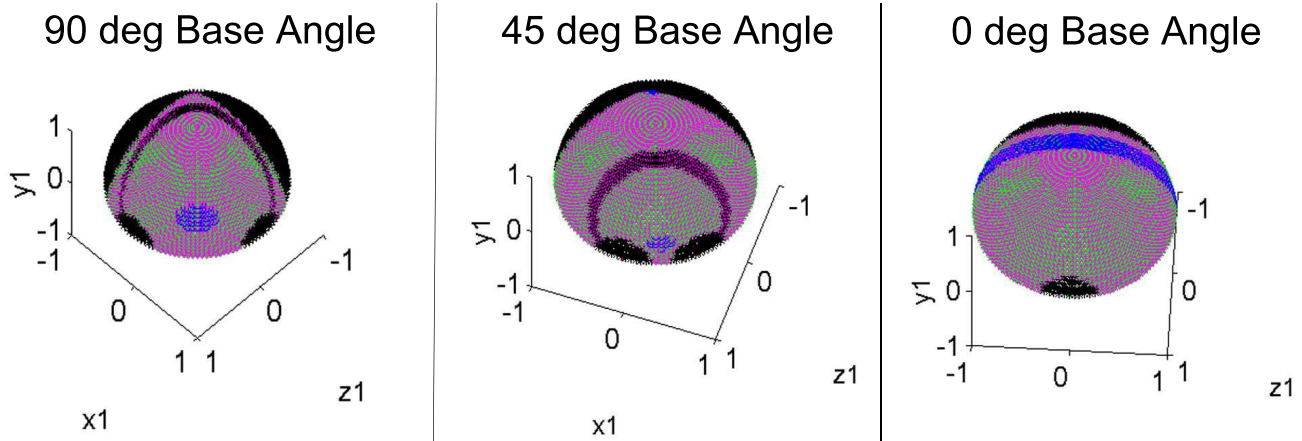


Fig. 4. The workspace is shown for the parallel mechanism with four equal link lengths of 60° as a function of three different base angle $\alpha_{12} = 90^\circ, 45^\circ, 0^\circ$. Black represents areas outside the reachable workspace or areas near kinematic singularity. The circular area in the center of the workspace for the 90° and 45° bases and the stripe for the 0° base represent an area of greatest isotropy. Notice that for the 90° and 45° bases and area of singularity cuts through the reachable workspace, a property that is highly undesirable.

4 It was shown both experimentally and analytically that the serial mechanism is better suited for a
 5 surgical manipulator. In this study, optimization criteria consisted of kinematic isotropy (the ratio of
 6 singular values of the Jacobian matrix) in the numerator and a link length penalty in the denominator.
 7 The combined criterion rewards good kinematic performance and penalizes size. With this criterion at its
 8 core, the optimization was performed comprehensively over the design space with all combinations of

1 each link ranging from 30° - 90° . Within each design candidate the target workspace was the DWS, the
2 60° cones. Only the designs that could also reach the EDWS were considered. The optimization resulted
3 in a design of 75° for the first link angle and 60° for the second link angle. The optimized link angles
4 served as the foundation for extensive mechanical design.

5 *3.1.2. Surgical Manipulators:* The 7-DOF cable-actuated surgical manipulator, shown in Figure 5, is
6 broken into three main pieces; the static base that holds all the motors, the spherical mechanism that
7 positions the tool, and the tool interface. The motion axes of the surgical robot are:

- 8 1) Shoulder Joint (rotational)
- 9 2) Elbow Joint (rotational)
- 10 3) Tool Insertion / Retraction (translational)
- 11 4) Tool Rotation (rotational)
- 12 5) Tool Grasping (rotational)
- 13 6) Tool Wrist-1 Actuation (rotational)
- 14 7) Tool Wrist-2 Actuation (rotational)

15 The first four joint axes intersect at the surgical port location, creating a spherical mechanism that
16 allows for tool manipulation similar to manual laparoscopy. The mechanism links are machined from
17 aluminum, and are generally I-section shapes with structural covers. These removable covers allow access
18 to the cable system, while improving the torsional stiffness of the links. The links are also offset from
19 the joint axis planes, allowing for a tighter minimum closing angle of the elbow joint.

20 The RAVEN utilizes DC brushless motors located on the stationary base, which actuate all motion
21 axes. Maxon EC-40 motors with 12:1 planetary gearboxes are used for the first three axes, which see the
22 highest forces. The first two axes, those under the greatest gravity load, have power-off brakes to prevent
23 tool motion in the event of a power failure. The fourth axis uses an EC-40 without a gearbox, and Maxon
24 EC-32 motors are used for the remaining axes. Maxon DES70/10 series amplifiers drive these brushless
25 motors. The motors are mounted onto the base via quick-change plates that allow motors to be replaced
26 without the need to disassemble the cable system.

27 The cable transmission system is comprised of a capstan on each motor, a pretension adjustment pulley,
28 various pulleys to redirect the cables through the links, and a termination point to each motion axis. The
29 shoulder axis is terminated on a single partial pulley. The elbow axis has a dual-capstan reduction stage
30 terminating on a partial pulley. The tool insertion / retraction axis has direct terminations of the cables

1 on the tool holder. The tool rotation, grasping and wrist cables are terminated on capstans on the tool
2 interface.

3 The cable system transmission ratios for positioning the tool tip are:

- 4 1) Shoulder: 7.7:1 (motor rotations: joint rotations)
- 5 2) Elbow: 7.3:1 (motor rotations: joint rotations)
- 6 3) Insertion: 133:1 (radians: meters)

7 Each axis is controlled by two cables, one for motion in each direction, and these two cables are
8 pretensioned against each other. The cables are terminated at each end to prevent any possibility of
9 slipping. The cable system maintains constant pretension on the cables through the entire range of motion.
10 Force and motion coupling between the axes is accommodated for in the control system.

11 Laser pointers attached to the shoulder and elbow joints allow for visual alignment of the manipulator
12 relative to the surgical port. When the two dots converge at the port location, the manipulator is positioned
13 such that its center of rotation is aligned with the pivot point on the abdominal wall. The power-off
14 brakes can be released by flipping a switch located on the base. The brakes are normally powered by
15 the control electronics, but also have a battery plug-in for easy set-up and break-down when the system
16 is not powered. ABS plastic covers were created on a 3D printer to encapsulate the motor pack thereby
17 protecting actuators, encoders and electrical wiring. Figure 7(a) shows the complete patient site.

18 The tool interface, shown in Figure 6, controls the tool rotation, grasp, and wrist axes, and allows
19 for quick changing of tools. The coupler is designed for one-handed engagement/disengagement of the
20 surgical tool to the manipulator. The tools used are Micro-Joint tools from the Zeus surgical robot that
21 have been adapted for use on the RAVEN. The tools' grasp and wrist axes are actuated by pushrods in
22 the tool shaft. High pitch acme threads in the tool interface convert the rotational motion of the cable
23 system capstans into linear motion of the tool pushrods. Because the modified Zeus tools only feature
24 one wrist axis, the surgical robot currently utilizes one of its two wrist axes.

25 3.2. *The Surgeon Site*

26 The surgeon site was developed to be low cost and portable, a choice that allows for easier telesurgical
27 collaboration. It consists of two PHANTOM Omni devices (SensAble Technologies, Woburn, MA), a
28 USB foot-pedal, a laptop running the surgeon's graphical user interface software, and a video feed of the
29 operative site as shown in Figure 7(b). SensAble's PHANTOM haptic devices are well established amongst

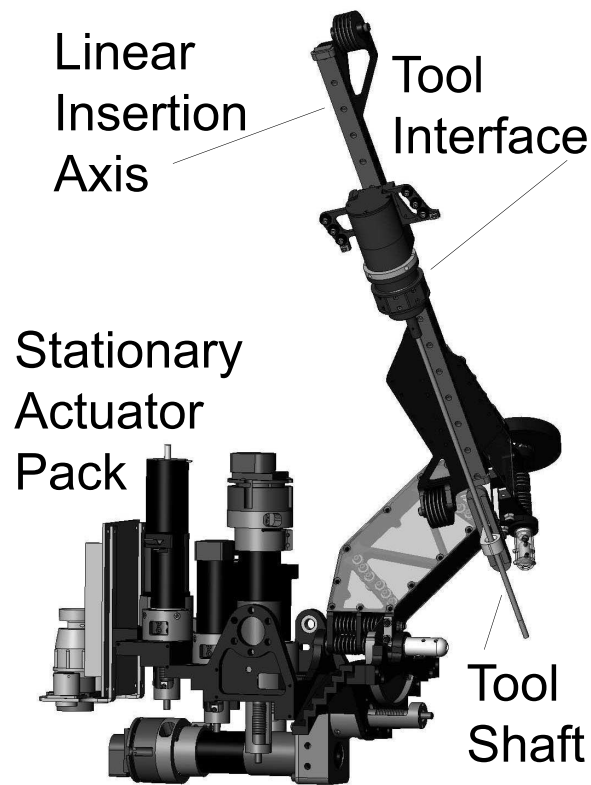


Fig. 5. CAD rendering of surgical manipulator shown with plastic covers removed. Mass: 12.3kg; folded dimensions 61cm x 53cm x 38cm; extended dimensions: 120cm x 30cm x 38cm.

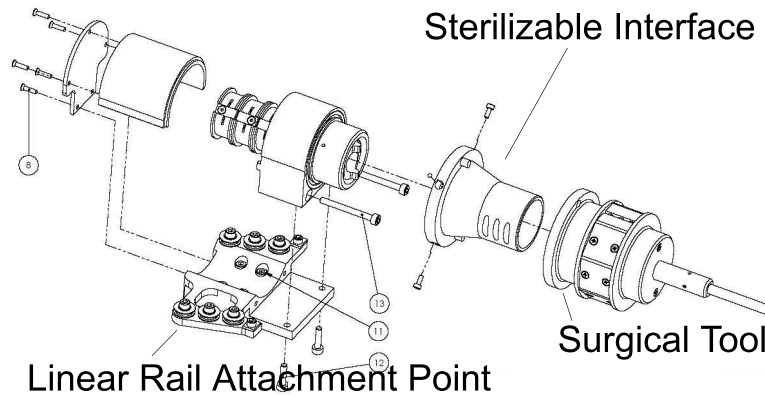


Fig. 6. Line drawing of tool interface, exploded view.

1 haptics researchers with a development environment that is straightforward to use. The Omni is a cost
 2 effective solution that allowed us to quickly implement a surgeon interface device for our master/slave
 3 system. It features 3-DOF force-feedback, 6-DOF sensing and two momentary switches on the stylus.
 4 The system does not currently utilize the force-feedback capability of the Omni. The foot-pedal enables
 5 and disables the coupling between the patient site and surgeon site allowing for position indexing.



Fig. 7. a) The RAVEN Patient Site and b) the Surgeon Site.

4. SOFTWARE AND CONTROL

4.1. Patient Site

Control software is running in the kernel space of an RTAI Linux computer at rate of 1kHz. The critical link between the control software and the motor controllers is a USB 2.0 interface board. Our USB board features eight channels of high-resolution 16bit D/A for control signal output to each controller and eight 24bit quadrature encoder readers.

4.1.1. Software and Safety Architecture: The control system and surrounding electronic hardware were designed to incorporate safety, modular design, and flexibility. As this is a medical device, the most critical of these aspects is safety. Inherent to a safe system is robustness, reliability, and some level of automatic override. To achieve reliability we defined four software states in which our system can operate: Initialization, Pedal Up, Pedal Down, and Emergency Stop (Figure 8). At power-up, the manipulators are resting against hard stops. The initialization state takes each manipulator from its resting position and moves it into the surgical field. Once the initialization is complete the system automatically transitions into the Pedal Up state. In the Pedal Up state the robot is not moving and brakes are engaged. The system enters Pedal Up when the surgeon lifts his/her foot from the foot-pedal, decoupling the master from the surgical manipulator. This is done to perform tool indexing or free the surgeon's hands for peripheral tasks. The Pedal Down state is initiated when the surgeon pushes the foot-pedal down, releasing the brakes and allowing the master device to directly control the surgical manipulator.

A Direct Logic 05 programmable logic controller (PLC) controls motor-enable, brakes, and the system states based on inputs received from the system. PLCs are a robust technology used extensively in

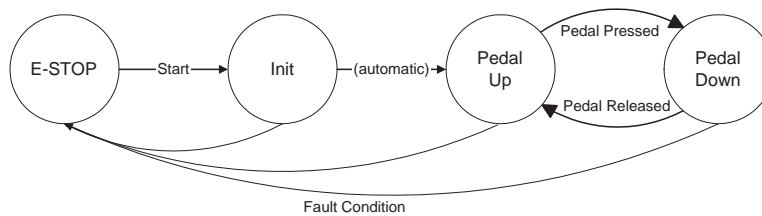


Fig. 8. Control System State Diagram.

1 automation applications. PLC technology is reliable and provides built-in, easy-to-use safety circuitry. In
 2 addition to monitoring the system hardware, the PLC monitors the state of the control software through
 3 the use of a watch-dog timer. The watch-dog timer monitors a square-wave signal generated by the control
 4 software, output from the parallel port of the Linux PC. In the event of a software or computer hardware
 5 failure, the PLC will detect the loss of the square-wave and immediately put the system into the Emergency
 6 Stop state, enabling the brakes and disabling the motors. An array of status LEDs displays the current
 7 state of the system. The RTAI Linux control software detects state transitions of the PLC and follows
 8 them within 1ms.

9 *4.1.2. Gravity Compensation:* Gravity introduces torques on the robot links that a control system has
 10 to combat to maintain a nominal pose, in addition to any environmental forces encountered by the end-
 11 effector. A model-less, closed-loop control system, such as PID, does not take these gravitational effects
 12 into account. While a closed loop controller can compensate to an extent for this disturbance effect,
 13 its ability to respond to movement commands is degraded by the additional load. By adding gravity
 14 compensation, the controller responds only to user input, and the system is more responsive. Only the
 15 first two joints of the RAVEN require compensation for gravity; the last four have enough friction that
 16 gravity does not significantly effect their dynamics.

17 The direct Lagrangian method was employed to calculate the expected gravity torque on each link
 18 [Checcacci et al., 2002]. Potential energy of the RAVEN robot links can be given by:

$$E_p = -m_1[{}^0g^T][{}^0R]_1[{}^1c_1] - m_2[{}^0g^T][{}^0R]_2[{}^2c_2] - m_3[{}^0g^T]({}^0l_3 + [{}^0R]_3[{}^3c_3])$$

19 where E_p is the potential energy of the system, m_n is the mass of link n , and ${}^n c_n$ is the center of mass
 20 of link n described in a coordinate frame attached to that link. The mass and center of mass values are
 21 taken from the CAD models of the system. 0R_n is the rotation matrix describing the orientation of points
 22 in coordinate frame n , in coordinate frame 0. The rotation matrix is derived from the robot kinematics

1 equations. The gravity vector, described in the base frame, is given by 0g . Finally, 0l_3 is the insertion
 2 displacement of the tool-carriage, measured in the base frame.

3 The gravitational torque on a joint is the partial derivative of E_p with respect to that joint. The vector
 4 of gravity torques is then:

$$G(\Theta) = \frac{\partial E_p}{\partial \Theta} = \begin{bmatrix} \frac{\partial E_p}{\partial \theta_1} \\ \frac{\partial E_p}{\partial \theta_2} \\ \frac{\partial E_p}{\partial d_3} \end{bmatrix}$$

5 where Θ is a vector of the joint variables, θ_1 , θ_2 , and d_3 (tool carriage insertion). Using the first two
 6 elements above, the expected gravitational torques on links one and two, were added to the controller
 7 torque applied by the actuators. The RAVEN did not initially have gravity compensation, and the surgeons'
 8 response to this improvement has been overwhelmingly positive.

9 *4.1.3. Engineers' Interface:* The Engineers' Interface (EI), a low-level interface to the states and
 10 mechanisms of the control software, assists robot development. Developers are presented with an intuitive
 11 GUI with easy access to robot features. In development stages, the system run level (stop, init, run, e-stop)
 12 can be set manually with the click of a button. Control commands can be sent to any degree of freedom
 13 or the entire robot. For example, a 40° sine wave can be output on the shoulder joint, or motor controller
 14 number two can output 30% maximum current, or the end-effector position can be instructed to move
 15 3cm left. Furthermore, robot information (such as motor output, joint position, and end-effector position)
 16 is displayed on-screen in real-time, and also logged for later evaluation.

17 The EI can connect to the RTAI Linux control system using either FIFO device nodes or a single, bi-
 18 directional (TCP/IP) network socket. Two types of data are exchanged: a packet containing all robot-state
 19 information is received by the EI, and a command packet with all instruction parameters is sent from the
 20 EI to the control software. This link is independent of the master-slave link.

21 4.2. Surgeon Site

22 The Surgeon Site software provides the surgeon with a GUI to log-in and connect to the Patient Site.
 23 It allows for unique identification of each user, keeping a detailed log of when each user logs into the
 24 system, connects to the Patient Site and transitions between pedal-up and pedal-down states. It provides
 25 an automatic means by which each user's time on the system can be tracked.

5. EXPERIMENTS

The first teleoperation of the RAVEN took place on October 15, 2005 in a cross-campus demonstration at the University of Washington (UW) with the surgeon site in a lecture hall and the patient site in the BioRobotics Lab (BRL). The surgical manipulator's first three degrees of freedom; the shoulder, elbow and tool insertion joints were actuated. A PHANToM Omni was used to control the endpoint of the surgical tool through the UW's campus network with no noticeable delay.

The implementation of a low-cost and portable surgeon site has provided the opportunity for telesurgical collaboration. The telesurgery experiments summarized in Table I have included many topologies including within one lab, between labs, and mobile robotic telesurgery experiences. Figure 9 is a functional block diagram of the system, illustrating the key components of the patient site, the surgeon site, and the communication layer between them. The RAVEN has been tested in a variety of environments using a multiple communication layer topologies and has demonstrated its portability and robustness.

TABLE I
SUMMARY OF TELESURGERY EXPERIMENTS.

Experiment	Date(s)	Patient Site	Surgeon Site	Communication Layer	
				Video	Network Architecture
HAPs/MRT	June 5-9, 2006	Field, Simi Valley, CA	Field, Simi Valley, CA	HaiVision Hai560	Wireless via UAV
ICL	July 20, 2006	BioRobotics Lab, Seattle, WA	Imperial College, London, England	iChat or Skype	Commercial Internet
Animal Lab	March 8, 2007	CVES, Seattle, WA	CVES, Seattle, WA	Direct S-video	LAN
NEEMO Aquarius	May 8-9, 2007	Aquarius Undersea Habitat, 3.5 miles off Florida Keys, 60 ft depth	University of Washington, Seattle	HaiVision Hai1000	Commercial Internet between Seattle, WA and Key Largo, FL; microwave communication link across 10 miles, Key Largo to Aquarius
NEEMO NURC	May 12-13, 2007	National Undersea Research Center, Key Largo, FL	University of Washington, Seattle	HaiVision Hai200	Commercial Internet

5.1. High Altitude Platforms/Mobile Robotic Telesurgery (HAPs/MRT)

Many research systems live out their entire life cycle in a laboratory environment, from conception to decommission, and are never challenged to move outside of that environment. A testament to the RAVEN's robustness was its first field deployment that took place June 5-9 2006. Dr. Timothy Broderick, MD, Charles Doarn and Brett Harnett of the University of Cincinnati led the HAPs/MRT project to

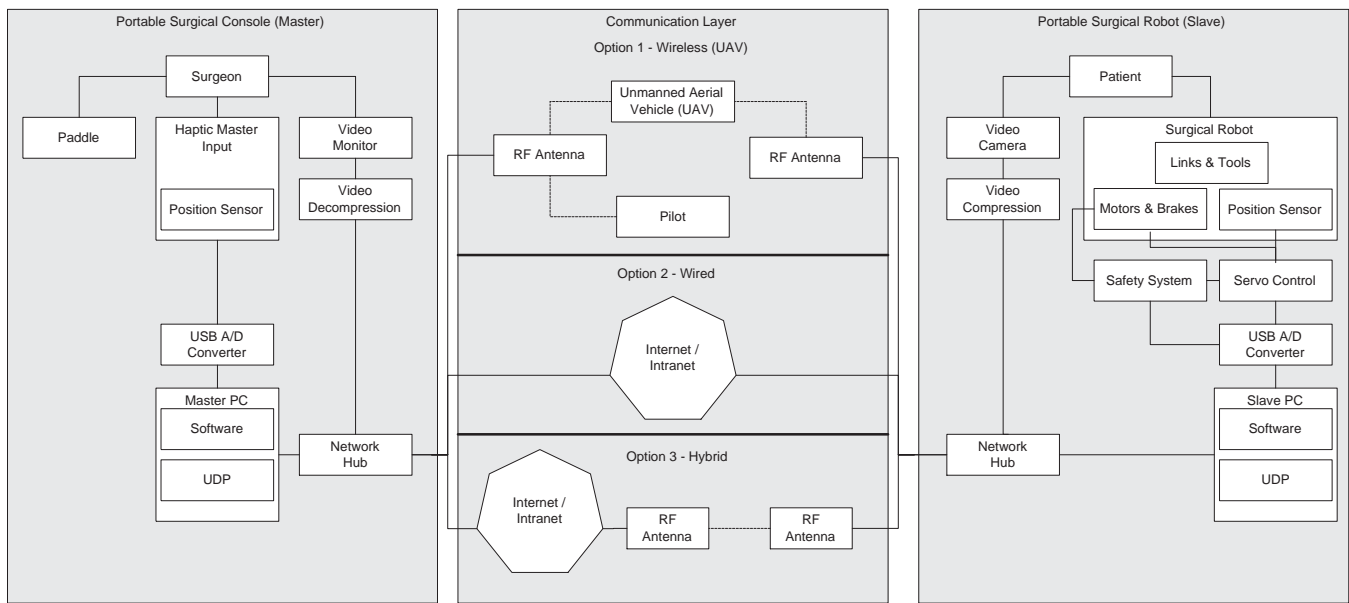


Fig. 9. RAVEN functional block diagram. The communication layer can take a few different forms including wireless UAV (HAPs/MRT), Wired (ICL, within lab experiments, animal lab), or hybrid (NEEMO) configurations.

1 evaluate surgical robotics in field conditions. As a collaborator in the HAPs/MRT project, the RAVEN
 2 was taken from the BRL in Seattle, WA and deployed in the desert of Simi Valley, CA for telesurgery
 3 experiments on an inanimate model (see Figure 12). The system was powered by gas generators and was
 4 set up under portable tents in an isolated field. Separated by a distance of 100 meters, the surgeon and
 5 patient sites were connected via an aerial digital datalink on board AeroVironment's PUMA unmanned
 6 aircraft. The datalink provided by AeroVironment utilized Internet-style communication at a rate of 1MB
 7 per second between the two sites, allowing the network architecture to remain unmodified. HaiVision Inc.
 8 (Montreal, Canada) provided a hardware codec that used MPEG-2 and transmitted the video signal at
 9 800kbps.

10 Two surgeons, Dr. Broderick and Dr. Lynn Huffman from the University of Cincinnati, performed a
 11 set of tasks including touching a series of landmarks and suturing on a gloved box. The gloved box was
 12 marked with a circle and a grid of landmarks spaced 1cm apart left to right and 0.5cm apart toward and
 13 away as shown in Figure 10(a). The landmarks were put in a numeric sequence starting with 1 at the
 14 upper left, 2 upper right, moving down through the rows, finishing at the lower right. The following five
 15 tasks were part of the experimental protocol:

- 16 1) Right tool touches each landmark in numeric order.
- 17 2) Left tool touches each landmark in numeric order.
- 18 3) Touch each landmark in numeric order using alternating left and right tool. Right tool touches the

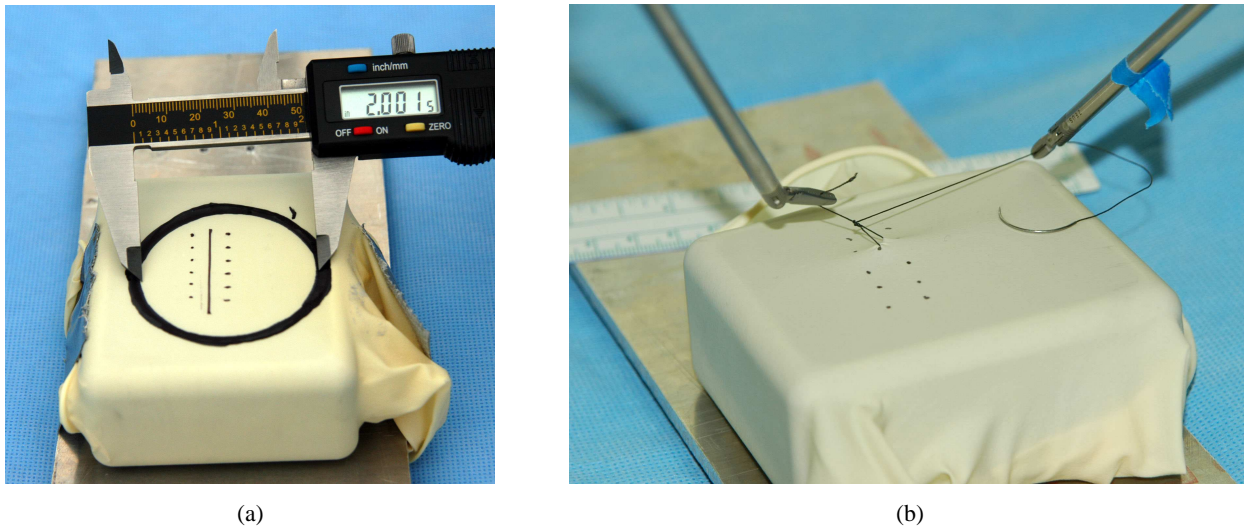


Fig. 10. (a) Experimental protocol was performed on a gloved box. (b) Successful suture tied on gloved box.

1 odd numbered landmarks (left column), left tool touches the even numbered ones (right column).

2 4) Right tool traces inner edge of circle in a clockwise direction.

3 5) Left tool traces inner edge of circle in a clockwise direction.

4 During three days of field deployment, kinematic data of the surgeons' commands and the surgical
 5 manipulators' motions were collected along with network characterization data. Figure 11 shows the
 6 tool tip path of Dr. Broderick touching each of the dots with his left hand. Deploying the system into
 7 a field environment and successfully executing the experimental protocol demonstrated the feasibility
 8 of performing Mobile Robotic Telesurgery (MRT) through a wireless communication link with limited
 9 bandwidth and variable time delays in an extreme or remote environment.

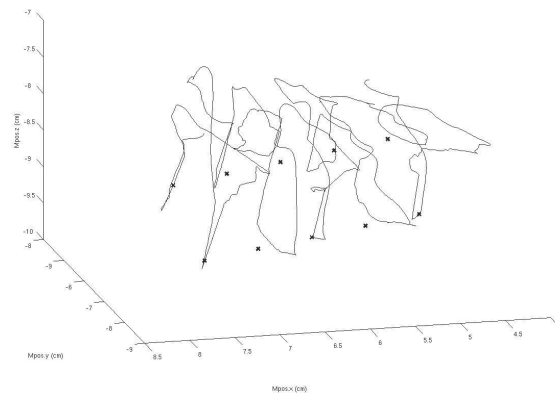


Fig. 11. Tool tip trajectory for Task 2 (touch each dot with left hand) while operating through UAV. The x's represent the location of each dot.



Fig. 12. Surgical robot system deployed in a remote field in Simi Valley, CA.

1 *5.2. Imperial College, London, England (ICL) to University of Washington, Seattle, WA, USA.*

2 In collaboration with Julian Leung, George Mylonas, Sir Ara Darzi and Ghuang Zhong Yang from
 3 Imperial College (London, England) we demonstrated the ability of the RAVEN to operate across a long
 4 distance. On July 20, 2006, in the lab in London, the surgeon site was set up with two PHANToM 6-DOF
 5 Premium haptic devices and our surgeon console software. iChat (Apple Computer Inc) was used for
 6 video feedback. The patient site was run from our lab in Seattle, WA. Time delay between the patient
 7 and surgeon sites was about 140 ms for Internet latency (measured by ping) and about 1 second for
 8 video encoding/decoding. This experiment showed that the master console software was general enough
 9 to adapt to other PHANToM devices, and also demonstrated the system's ability to teleoperate across long
 10 distances. During this experiment, the remote surgeons performed the same set of tasks on the gloved box
 11 as were performed during HAPs/MRT. Figure 13 shows the tool path of Dr. Leung tracing out the circle.

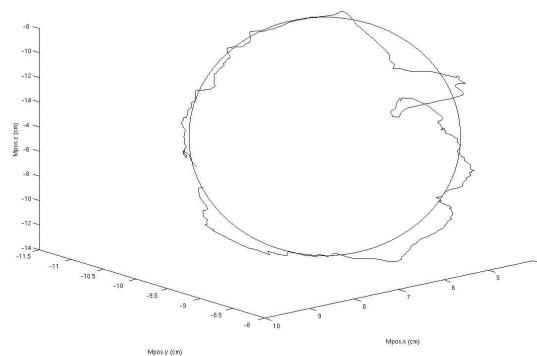


Fig. 13. Tool tip trajectory for Task 4 (trace the circle with right hand) while operating between Seattle, WA and London, England.

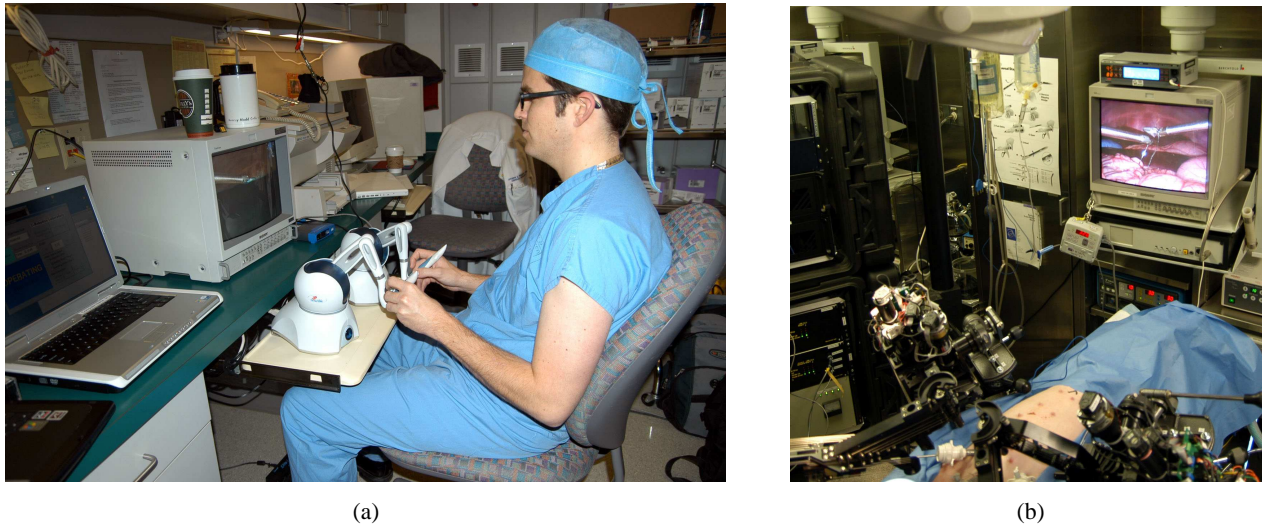


Fig. 14. (a) The surgeon controls (b) RAVEN and successfully ties a knot.

1 5.3. Animal Lab

2 On March 8, 2007, in collaboration with the University of Washington Center for Video Endoscopic
 3 Surgery (UW CVES), three surgeons performed surgical tasks on a live porcine model (UW-IACUC
 4 approval #2469-04, “Robotic Surgery”). The tasks involved measuring out a specified length of bowel as
 5 well tying a suture. The patient site was set up in the animal lab, with the surgeon site in an adjacent
 6 office. Video feedback was sent directly through an S-video cable that ran between the two rooms. Figure
 7 14 shows the surgeon in one room tying a suture on a piece of bowel, with the patient in the next room.
 8 This experiment was a step toward proving that the RAVEN could operate on a real patient, not just on
 9 dry lab task boards.

10 5.4. NASA Extreme Environment Mission Operations (NEEMO) XII

11 5.4.1. TeleRobotic FLS: In the area of surgical robotics there is no clinically relevant testing standard.
 12 As we did in HAPs/MRT and with our Imperial College collaborations, each set of researchers devises
 13 their own experimental protocol by which to test their system. The same was true in surgery until the
 14 late 1990s when the Society of American Gastrointestinal and Endoscopic Surgeons (SAGES) created
 15 a committee to develop curriculum for teaching the Fundamentals of Laparoscopic Surgery (FLS). The
 16 outcome is a curriculum that includes both cognitive and psychomotor skills. The FLS skills tasks have
 17 been validated to show significant correlation between score and postgraduate year [Derosis et al., 1998].
 18 These tasks have been used to quantitatively assess the skill of thousands of surgeons ranging from novice
 19 to expert and are considered by many the “gold standard” in surgical skill assessment.

1 To move toward a standard for surgical robot evaluation and testing, we have adopted the FLS skills
 2 tasks to use in our experiments. The NASA NEEMO XII mission was our first use of the new task set,
 3 with the FLS Peg Board Transfer (aka Block Transfer) task, shown in Figure 15, chosen as the primary
 4 skills task. In the SAGES implementation of this task, the surgeon uses MIS graspers to move all six
 5 blocks from one side to the other then back. The order does not matter, but blocks picked up on the left
 6 must be picked up with the left tool, transferred in the air to the right tool, and then set down on any peg
 7 on the right (and vice versa). The score is a proprietary formula based on completion time for the task
 8 as well as the number of errors (errors defined as a block dropped outside the black boundaries (shown in
 9 Figure 15)). The TeleRobotic FLS Block Transfer in contrast is more structured. The pegs are numbered
 10 and blocks must be transferred in order from left to right then right to left. The time to transfer each
 11 block is recorded for a total of twelve block transfer times per trial. Errors are classified as either Type
 12 1 (dropped and recovered) or Type 2 (dropped and not recovered). The data reported are mean block
 13 transfer time as well as the number of each type of error.

14 *5.4.2. NEEMO Experiments:* On May 7, 2007 the RAVEN began its 3-day deployment as part of the
 15 large-scale 12-day training exercise. The NEEMO missions are training analogs to space flight that train
 16 not only astronauts but also support personnel on how to run missions. These missions take place in the
 17 Florida Keys at the National Undersea Research Center (NURC) in Key Largo, FL and at the Aquarius
 18 Undersea Habitat, 3.5 miles offshore at a depth of 60 feet.

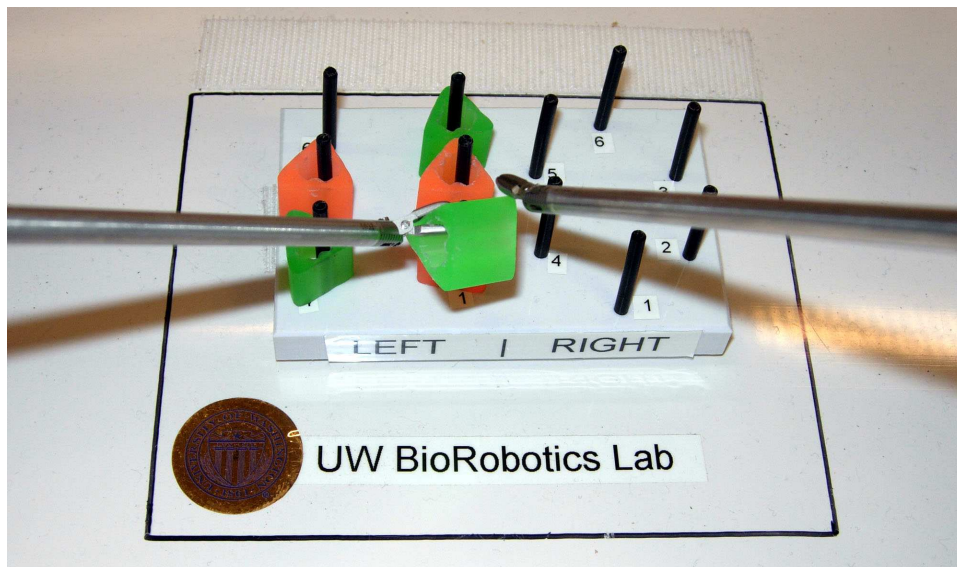


Fig. 15. The SAGES FLS Block Transfer task board set up with the RAVEN moving a block from left to right.

19 During our experiment, the surgeon site was set up in a conference room in Seattle, WA. The patient

1 site was set up and supported by two surgeons inside Aquarius. Communication between the patient
2 and surgeon sites travelled between UW and NURC via commercial Internet, then from NURC across a
3 wireless microwave communication link to the Life Support Buoy, and down a hardwired umbilical into
4 Aquarius.

5 In order to gather network performance characteristics, a UDP packet reflector program was placed at
6 the servers at NURC and Aquarius in Florida. The UDP packet reflector program receives the UDP data
7 packets and routes them to back to the sender, in this case, back to our workstation at the UW. A similar
8 UDP data structure used in the telesurgery experiments were used for the performance measurements.
9 Each UDP data packet was time stamped at the workstation in UW and sent to the servers at NURC and
10 Aquarius and the reflected packets were used to measure the elapsed round-trip time between the two
11 locations. UDP packet sequence number was also used to measure the number of lost and out-of-sequence
12 packets during the tests.

13 6. RESULTS

14 The RAVEN was conceived from a close collaboration between engineers and surgeons. The system
15 is a new platform for telesurgery experiments. Table II summarizes the mean network latency during five
16 different experiments. The total delay experienced by the surgeon during teleoperation is a function of both
17 network latency as well as video compression and decompression times. Depending on the video codec
18 used video latency can vary dramatically and is difficult to measure accurately. During these telesurgery
19 experiments, data to characterize the network conditions was collected. Figure 16 shows a histogram of
20 the network conditions during NEEMO.

21 The SAGES FLS skills tasks are well defined and the kit readily available for purchase. Developing a
22 “Telerobotic FLS” protocol will give consistency to telesurgical experiments. Figure 17 summarizes the
23 mean completion time for expert surgeon E1 performing the Block Transfer task. In each of the first
24 three weeks of training, E1 performed three repetitions of the Block Transfer in the lab environment with
25 effectively no delay. There is a learning effect as E1’s mean time improved from week to week. During
26 the NEEMO mission, there was limited time, so E1 was only able to complete a single repetition with
27 the RAVEN in Aquarius and another single repetition with it on-shore in Key Largo. While these results
28 do not show statistical significance, one can observe a learning effect most likely due to accommodating
29 for telesurgery latency. For comparison, the same surgeon, who uses a da Vinci clinically, was able to

TABLE II
SUMMARY OF EXPERIMENTS, MEAN NETWORK LATENCY AND SIGNIFICANCE OF EACH.

Experiment	Mean Network Latency (ms)	Significance
HAPs/MRT	16	Operated in a field environment to test ruggedness and portability. Communicated via wireless through a UAV.
ICL	172	Adaptability of surgeon site to other Sensable devices. Teleoperation over long distance.
Animal Lab	1	Demonstrated ability to operate on a real patient through MIS ports.
NEEMO Aquarius	76	Telerobotic FLS for performance measurement. Operating in a unique environment. Communicating across both commercial Internet and long distance wireless.
NEEMO NURC	75	Additional opportunity to collect Telerobotic FLS data over long communication network.

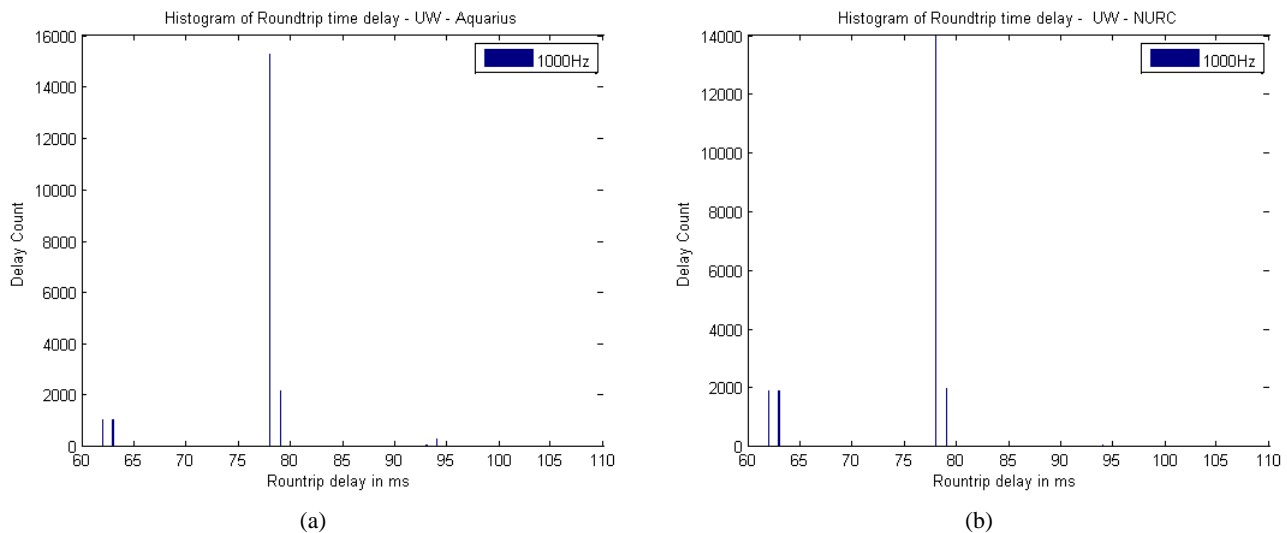


Fig. 16. Histogram of packets with respect to delay between (a) UW and Aquarius and (b) UW and NURC.

1 complete the block transfer task in about one minute using the da Vinci, taking only slightly longer with
 2 the stereo capability disabled. The da Vinci results are also included in Figure 17.

3 7. CONCLUSIONS

4 Starting with an extensive database of *in-vivo* minimally invasive surgical measurements, the require-
 5 ments for tissue manipulation and tool handling were defined. Using a clinically relevant design specifi-
 6 cation, a kinematic optimization was performed on a spherical mechanism to obtain the ideal link lengths
 7 for the surgical manipulator. The mechanical design of the manipulators minimizes inertia through careful
 8 design of the link structure and placement of all the actuators on a stationary base. RTAI-based control
 9 software was developed in conjunction with a USB-interface board allowing for high performance real-

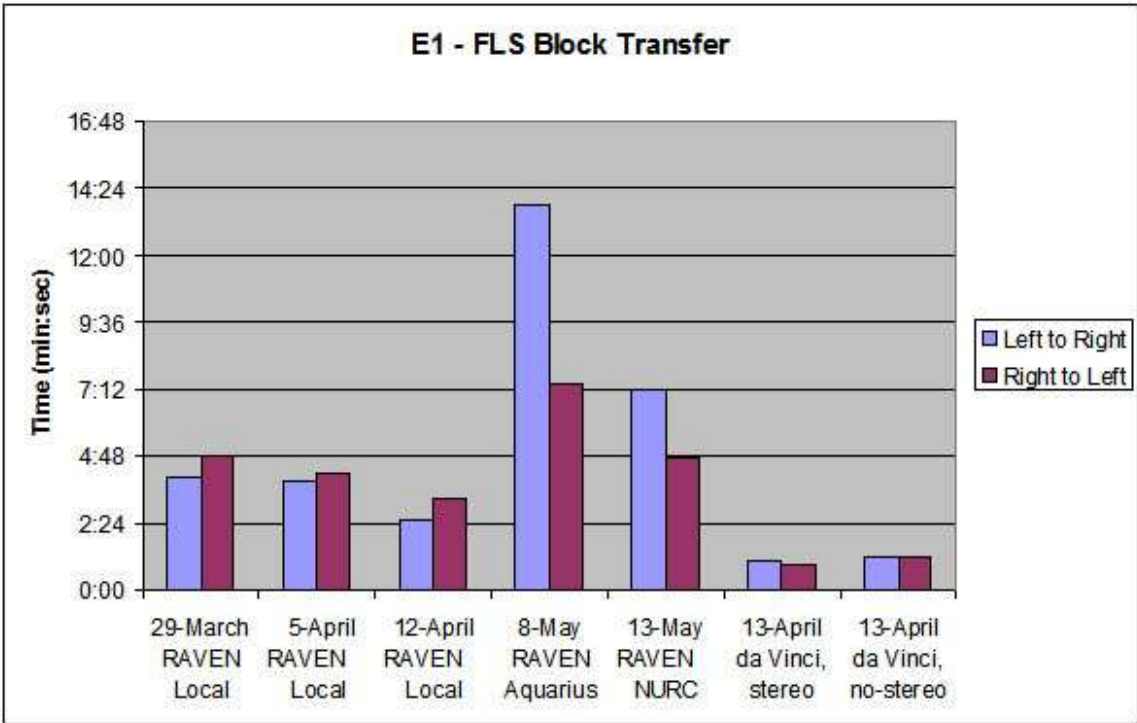


Fig. 17. Average block transfer completion times of surgeon E1 during local training on the RAVEN as well as during the NEEMO mission. Completion times using an ISI da Vinci are included for comparison.

1 time control of the system. Integrating commercially available haptic devices into the surgeon console
 2 provided an inexpensive solution to surgeon site control of the surgical manipulators and enabled many
 3 collaboration opportunities. We have created a platform upon which further telesurgery experiments will
 4 be based.

5 **8. FUTURE DEVELOPMENT**

6 *8.1. TeleRobotic FLS*

7 Successful completion of multiple teleoperation experiments has demonstrated the system’s ability to
 8 perform both within our own lab as well as in extreme environments. In these teleoperation experiments,
 9 time delay was a challenge for the remote surgeon to overcome. From our initial experiments it is clear
 10 there is a distinct learning effect when performing a relatively simple task with the RAVEN. A training
 11 protocol has been developed to study learning on the RAVEN. Further studies will investigate surgeons
 12 performing SAGES FLS tasks under a variety of emulated time delay and network conditions. Knowledge
 13 of how surgeons adapt and perform under time delay will greatly impact the future of telesurgery.

1 8.2. Bilateral Teleoperation

2 One of the many goals of robotic surgery is to provide the surgeon with an augmented sense of touch.
 3 Bilateral teleoperation, or force feedback, is a challenging problem. A large obstacle that has been the
 4 subject of separate research is force feedback teleoperation across long distances with time delay. The
 5 RAVEN currently does not have direct force or position sensing at the tool tip. Position measurement
 6 is taken at the actuator with the tool tip position inferred from the kinematics of the system, but this
 7 measurement does not take into account the compliance of the cable actuation system or the flexibility
 8 of the long and slender MIS tools. Force/torque sensors that are small enough to pass through the MIS
 9 port and are sterilizable would be a vast improvement to the sensing problem.

10 ACKNOWLEDGMENTS

11 Development of the RAVEN was supported by the US Army, Medical Research and Materiel Com-
 12 mand, grant number DAMD17-1-0202. The HAPs/MRT project was supported by the US Army, Medical
 13 Research and Materiel Command grant number W81XWH-05-2-0080. The authors would like to thank
 14 our HAPs/MRT collaborators at the University of Cincinnati, AeroVironment, and HaiVision as well as
 15 our collaborators in London at Imperial College. The NEEMO XII participation has been supported by
 16 the US Army TATRC grant number W81XWH-07-2-0039. The authors would like to thank our NEEMO
 17 collaborators from University of North Carolina at Wilmington, US Navy, National Undersea Research
 18 Center, National Oceanographic and Atmospheric Administration, NASA, and the University of Cincinnati.

19 REFERENCES

- 20 [Berkelman et al., 2003] Berkelman, P., Boidard, E., Cinquin, P., and Troccaz, J. (2003). LER: The Light Endoscope Robot. *IEEE/RSJ*
 21 *International Conference on Intelligent Robots and Systems*, 3:2835–2840.
- 22 [Cavusoglu et al., 2003] Cavusoglu, M., Williams, W., Tendick, F., and Sastry, S. (2003). Robotics for telesurgery: second generation
 23 Berkeley/UCSF laparoscopic telesurgical workstation and looking towards the future applications. *Industrial Robot*, 30(1):22–29.
- 24 [Checcacci et al., 2002] Checcacci, D., Sotgiu, E., Frisoli, A., Avizzano, C., and Bergamasco, M. (2002). Gravity compensation algorithms
 25 for parallel haptic interface. *Robot and Human Interactive Communication, 2002. Proceedings. 11th IEEE International Workshop on*,
 26 pages 140–145.
- 27 [Cleary and Nguyen, 2001] Cleary, K. and Nguyen, C. (2001). State of the Art in Surgical Robotics: Clinical Applications and Technology
 28 Challenges. *Computer Aided Surgery*, 6(6):312–328.
- 29 [Davies, 2000] Davies, B. (2000). A review of robotics in surgery. *Proceedings of the Institution of Mechanical Engineers, Part H: Journal*
 30 *of Engineering in Medicine*, 214(1):129–140.
- 31 [Davies et al., 1989] Davies, B., Hibberd, R., Coptcoat, M., and Wickham, J. (1989). A surgeon robot prostatectomy—a laboratory evaluation.
 32 *Journal of Medical Engineering and Technology*, 13(6):273–277.

- 1 [Derosis et al., 1998] Derosis, A., Fried, G., Abrahamowicz, M., Sigman, H., Barkun, J., and Meakins, J. (1998). Development of a model
2 for training and evaluation of laparoscopic skills. *American Journal of Surgery*, 2175.
- 3 [Ghodoussi et al., 2002] Ghodoussi, M., Butner, S., and Wang, Y. (2002). Robotic Surgery - The Transatlantic Case. *IEEE International*
4 *Conference on Robotics and Automation*, 2:1882–1888.
- 5 [Guthart and Salisbury, 2000] Guthart, G. and Salisbury, J.K., J. (2000). The Intuitive Telesurgery System: Overview and Application. *IEEE*
6 *International Conference on Robotics and Automation*, 1:618–621.
- 7 [Harris et al., 1997] Harris, S., Arambula-Cosio, F., Mei, Q., Hibberd, R., Davies, B., Wickham, J., Nathan, M., and Kundu, B. (1997). The
8 Probot-an active robot for prostate resection. *Proceedings of the Institution of Mechanical Engineers, Part H: Journal of Engineering in*
9 *Medicine*, 211:317–325.
- 10 [Hill et al., 1994] Hill, J., Green, P., Jensen, J., Gorfou, Y., and Shah, A. (1994). Telepresence Surgery Demonstration System. *IEEE*
11 *International Conference on Robotics and Automation*, 3:2302–2307.
- 12 [Hongo et al., 2002] Hongo, K., Kobayashi, S., Kakizawa, Y., Koyama, J., Goto, T., Okudera, H., Kan, K., Fujie, M., Iseki, H., and
13 Takakura, K. (2002). NeuRobot: Telecontrolled Micromanipulator System for Minimally Invasive Microneurosurgery-Preliminary Results.
14 *Neurosurgery*, 51(4):985–988.
- 15 [Jacobs, 1997] Jacobs, L. (1997). Determination of the learning curve of the AESOP robot. *Surgical Endoscopy*, 11(1):54–55.
- 16 [Kobayashi et al., 1999] Kobayashi, E., Masamune, K., Sakuma, I., Dohi, T., and Hashimoto, D. (1999). A New Safe Laparoscopic
17 Manipulator System with a Five-Bar Linkage Mechanism and an Optical Zoom. *Computer Aided Surgery*, 4(4):182–192.
- 18 [Kwoh et al., 1988] Kwoh, Y., Hou, J., Jonckheere, E., and Hayati, S. (1988). A Robot with Improved Absolute Positioning Accuracy for
19 CT Guided Stereotactic Brain Surgery. *IEEE Transactions on Biomedical Engineering*, 35(2):153–160.
- 20 [Lavallée et al., 1992] Lavallée, S., Troccaz, J., Gaborit, L., Cinquin, P., Benabid, A., and Hoffmann, D. (1992). Image guided operating
21 robot: a clinical application in stereotactic neurosurgery. *IEEE International Conference on Robotics and Automation*, 1:618–624.
- 22 [Lum, 2004] Lum, M. (2004). Kinematic Optimization of a 2-DOF Spherical Mechanism for a Minimally Invasive Surgical Robot. Master's
23 thesis, University of Washington.
- 24 [Lum et al., 2006] Lum, M., Rosen, J., Sinanan, M., and Hannaford, B. (2006). Optimization of a Spherical Mechanism for a Minimally
25 Invasive Surgical Robot: Theoretical and Experimental Approaches. *IEEE Transactions on Biomedical Engineering*, 53(7):1440–1445.
- 26 [Madhani et al., 1998] Madhani, A., Niemeyer, G., and Salisbury, J. (1998). The Black Falcon: A Teleoperated Surgical Instrument for
27 Minimally Invasive Surgery. *IEEE/RSJ International Conference on Intelligent Robots and Systems*, 2:936–944.
- 28 [Marescaux et al., 2001] Marescaux, J., Leroy, J., Gagner, M., Rubino, F., Mutter, D., Vix, M., Butner, S., and Smith, M. (2001). Transatlantic
29 robot-assisted telesurgery. *Nature*, 413:379–80.
- 30 [Mitsubishi et al., 2003] Mitsubishi, M., Arata, J., Tanaka, K., Miyamoto, M., Yoshidome, T., Iwata, S., Hashizume, M., and Warisawa, S.
31 (2003). Development of a Remote Minimally-Invasive Surgical System with Operational Environment Transmission Capability. *IEEE*
32 *International Conference on Robotics and Automation*, 2:2663–2670.
- 33 [Robinson and Stiegmann, 2004] Robinson, T. and Stiegmann, G. (2004). Minimally Invasive Surgery. *Endoscopy*, 36(1):48–51.
- 34 [Rosen et al., 2006] Rosen, J., Brown, J., Chang, L., Sinanan, M., and Hannaford, B. (2006). Generalized Approach for Modeling Minimally
35 Invasive Surgery as a Stochastic Process Using a Discrete Markov Model. *IEEE Transactions on Biomedical Engineering*, 53(3):399–413.
- 36 [Rovetta et al., 1996] Rovetta, A., Sala, R., Wen, X., and Togno, A. (1996). Remote Control in Telerobotic Surgery. *IEEE Transactions on*
37 *Systems, Man, and Cybernetics Part A: Systems and Humans*, 26(4):438–444.
- 38 [Sackier et al., 1997] Sackier, J., Wooters, C., Jacobs, L., Halverson, A., Uecker, D., and Wang, Y. (1997). Voice Activation of a Surgical
39 Robotic Assistant. *The American Journal of Surgery*, 174(4):406–409.

- 1 [Sim et al., 2006] Sim, H., Yip, S., and Cheng, C. (2006). Equipment and technology in surgical robotics. *World Journal of Urology*,
2 24(2):128–135.
- 3 [Taylor et al., 1995] Taylor, R., Funda, J., Eldridge, B., Gomory, S., Gruben, K., LaRose, D., Talamini, M., Kavoussi, L., and Anderson, J.
4 (1995). A Telerobotic Assistant for Laparoscopic Surgery. *IEEE Engineering in Medicine and Biology Magazine*, 14(3):279–288.
- 5 [Taylor et al., 1994] Taylor, R., Mittelstadt, B., Paul, H., Hanson, W., Kazanzides, P., Zuhars, J., Williamson, B., Musits, B., Glassman,
6 E., and Bargar, W. (1994). An Image-Directed Robotic System for Precise Orthopaedic Surgery. *IEEE Transactions on Robotics and*
7 *Automation*, 10(3):261–275.
- 8 [Taylor et al., 1989] Taylor, R., Paul, H., Mittelstadt, B., Glassman, E., Musits, B., and Bargar, W. (1989). Robotic Total Hip Replacement
9 Surgery in Dogs. *International Conference of the IEEE Engineering in Engineering in Medicine and Biology Society*, 3:887–889.
- 10 [Zemiti et al., 2007] Zemiti, N., Morel, G., Ortmaier, T., and Bonnet, N. (2007). Mechatronic Design of a New Robot for Force Control in
11 Minimally Invasive Surgery. *IEEE/ASME Transactions on Mechatronics*, 12(2):143–153.